Leukemia (2014) **28,** 770–778

www.nature.com/leu

OPEN

ORIGINAL ARTICLE

CBFB–MYH11/RUNX1 together with a compendium of hematopoietic regulators, chromatin modifiers and basal transcription factors occupies self-renewal genes in inv(16) acute myeloid leukemia

A Mandoli[1], AA Singh[1], PWTC Jansen[2], ATJ Wierenga[3,4], H Riahi[1], G Franci[5], K Prange[1], S Saeed[1], E Vellenga[3], M Vermeulen[2], HG Stunnenberg[1] and JHA Martens[1]

Different mechanisms for CBFβ–MYH11 function in acute myeloid leukemia with inv(16) have been proposed such as tethering of RUNX1 outside the nucleus, interference with transcription factor complex assembly and recruitment of histone deacetylases, all resulting in transcriptional repression of RUNX1 target genes. Here, through genome-wide CBFβ–MYH11-binding site analysis and quantitative interaction proteomics, we found that CBFβ–MYH11 localizes to RUNX1 occupied promoters, where it interacts with TAL1, FLI1 and TBP-associated factors (TAFs) in the context of the hematopoietic transcription factors ERG, GATA2 and PU.1/SPI1 and the coregulators EP300 and HDAC1. Transcriptional analysis revealed that upon fusion protein knockdown, a small subset of the CBFβ–MYH11 target genes show increased expression, confirming a role in transcriptional repression. However, the majority of CBFβ–MYH11 target genes, including genes implicated in hematopoietic stem cell self-renewal such as *ID1*, *LMO1* and *JAG1*, are actively transcribed and repressed upon fusion protein knockdown. Together these results suggest an essential role for CBFβ–MYH11 in regulating the expression of genes involved in maintaining a stem cell phenotype.

Leukemia (2014) **28,** 770–778; doi:10.1038/leu.2013.257

Keywords: CBFβ–MYH11; RUNX1; histone acetylation; acute myeloid leukemia; inv(16)

INTRODUCTION

Core-binding transcription factors (CBFs) have roles in stem cell self-renewal, tissue differentiation and cancer.[1] They are heterodimeric complexes consisting of two subunits, alpha and beta, in which the alpha subunit binds to DNA and is encoded by one of the *RUNX1* (*AML1, CBFα2*), *RUNX2* (*CBFα1*) and *RUNX3* (*CBFα3*) genes, whereas the beta subunit (CBFβ) is thought not to bind to DNA but to stabilize the DNA binding of the alpha subunit. RUNX1 is the CBF alpha subunit that is predominantly expressed during hematopoietic development, and both RUNX1 and CBFβ are frequently involved in chromosomal alterations associated with hematopoietic diseases, for example, in t(8;21) and inv(16) acute myeloid leukemia (AMLs).[2]

The translocation involving chromosomes 8 and 21 fuses the *RUNX1* and the *ETO* genes, leading to the expression of AML1-ETO. Expression of the AML1-ETO oncofusion protein in hematopoietic cells results in a stage-specific arrest of maturation and increased cell survival, predisposing cells to develop leukemia.[3] Whereas the AML1-ETO translocation is usually observed in AML subtype M2, the inversion of chromosome 16, inv(16)(p13q22), is associated with AML-M4Eo.[4] This inversion generates a chimeric gene *CBFβ–MYH11*, which encodes a fusion protein between CBFβ and smooth muscle myosin heavy chain (SMMHC/MYH11).[5–8]

Heterozygous *Cbfβ-Myh11* knock-in mice are embryonic lethal, with definitive hematopoiesis blocked at the stem-cell level. Moreover, adult hematopoietic stem cells fail to differentiate to myeloid and lymphoid lineages,[9] a phenotype similar to that of *Runx1*$^{-/-}$ and *Cbfβ*$^{-/-}$ mice[10,11] and suggesting that CBFβ-MYH11 is a dominant repressor of RUNX1/CBFβ function. Still, mutagenesis studies using *Cbfβ*$^{+/MYH11}$ knock-in mice indicate that CBFβ-MYH11 is necessary, but not sufficient, for leukemogenesis[12,13] and that additional genetic events, for example, c-KIT, RAS pathway or NDE1 mutations[14–17] are required for the onset of the disease.

At the molecular level, CBFβ–MYH11 has been suggested to exert its transcriptional regulator functions by several mechanisms. These include altering the normal RUNX1 transcription program through the tethering of RUNX1 outside the nucleus, interfering with transcription factor assembly, recruitment of histone deacetylases and inhibiting the RUNX1 activity.[4,18–20] However, many of these studies were based on *in vitro* and overexpression experiments. In addition, *in vivo* studies were hampered by the lack of knowledge on high-confidence binding sites of CBFβ–MYH11 and identification of the target gene program.

Here we performed genome-wide-binding analysis in cell lines and patient blasts and identified many previously unknown

[1]Department of Molecular Biology, Faculty of Science, Nijmegen Centre for Molecular Life Sciences, Radboud University, Nijmegen, The Netherlands; [2]Department of Molecular Cancer Research, UMC Utrecht, Utrecht, The Netherlands; [3]Department of Hematology, University of Groningen and University Medical Center Groningen, Groningen, The Netherlands; [4]Department of Laboratory Medicine University of Groningen and University Medical Center Groningen, Groningen, The Netherlands and [5]Dipartimento di Biochimica, Biofisica e Patologia Generale, Seconda Università degli Studi di Napoli, Napoli, Italy. Correspondence: Dr JHA Martens, Department of Molecular Biology, Faculty of Science, Nijmegen Centre for Molecular Life Sciences, Radboud University, PO Box 9101, Nijmegen, HB 6500, The Netherlands.
E-mail: j.martens@ncmls.ru.nl
Received 27 June 2013; revised 19 August 2013; accepted 22 August 2013; accepted article preview online 4 September 2013; advance online publication, 27 September 2013

CBFβ–MYH11-binding sites. In addition, we used mass spectrometry to identify new interactors of the CBFβ–MYH11/RUNX1 complex. We show that CBFβ–MYH11 binds DNA in a RUNX1-dependent manner and preferentially localizes to promoter regions. In addition, our study reveals that CBFβ–MYH11 operates in the context of a hematopoietic regulator complex consisting of various transcription factors linked to transcriptional activation. Finally, our study reveals that, in contrast to previous suggestions of CBFβ–MYH11 functioning as a transcriptional repressor, CBFβ–MYH11 binding can also be linked to transcriptional activation.

MATERIALS AND METHODS

Chromatin immunoprecipitation (ChIP)

Patient cells and cell lines (see Supplementary Information) were cross-linked with 1% formaldehyde for 20 min at room temperature, quenched with 0.125 M glycine and washed. Sonicated chromatin (Bioruptor, Diagenode, Liege, Belgium) was centrifuged at maximum speed for 10 min and then incubated with specific antibodies. Beads were washed sequentially with four different wash buffers and chromatin was eluted from the beads. Protein–DNA crosslinks were reversed, after which DNA was isolated and used for quantitative PCR or sequencing analysis.

Illumina high-throughput sequencing

End repair was performed using the precipitated DNA of ~6 million cells (3-4 pooled biological replicas) using Klenow and T4 polynucleotide kinase (T4 PNK). A 3′ protruding A base was generated using Taq polymerase and adapters were ligated. The DNA was loaded on gel and a band corresponding to ~300 bp (ChIP fragment + adapters) was collected. The DNA was isolated, amplified by PCR and used for cluster generation on the Illumina GAII or HiSeq genome analyzer. The 35–45 bp tags were mapped to the reference human genome using the Burrows-Wheeler Alignment Tool (BWA) or eland program allowing one mismatch. For each base pair in the genome, the number of overlapping sequence reads was determined, averaged over a 10 bp window and visualized in the UCSC genome browser (http://genome.ucsc.edu). All ChIP-seq and RNA-seq data can be downloaded from Gene Expression Omnibus accession number GSE46044, and the bioinformatic analysis of the data is described in the Supplementary Information.

SILAC labeling, pulldown and LC-MS/MS (liquid chromatography-mass spectrometry) analysis

ME-1 cells were SILAC (Stable Isotopes Labeling by Amino Acids in Cell Culture) labeled using RPMI1640 (-Arg, -Lys) medium (Gibco/Invitrogen, Paisley, UK) supplemented with either $^{13}C_6^{15}N_4$ L-arginine and $^{13}C_6^{15}N_2$ L-lysine (Isotec, Sigma, St Louis, MO, USA) or non-labeled L-arginine and L-lysine. Cells were cultured in SILAC medium for at least eight doublings to ensure full incorporation of the labeled amino acids. Nuclear extract preparation and pulldown were performed as previously described.[21]

RESULTS

CBFβ–MYH11 binding to DNA is RUNX1 dependent

CBFβ–MYH11 is the oncofusion protein that results from an inversion on chromosome 16. The oncogenic activities of this protein are thought to be related to its binding to RUNX1 (also named CBFα2 or AML1), thereby altering its function. Indeed, coimmunoprecipitation experiments using ME-1 cells,[22] which express the CBFβ–MYH11 variant type A, show that RUNX1 interacts with CBFβ–MYH11 (Figure 1a). CBFβ–MYH11 has also been suggested to be localized both inside as well as outside the nucleus thereby diverting RUNX1 out of the nucleus and altering the normal RUNX1 transcription program.[4] To examine the cellular localization of CBFβ–MYH11, we fractionated ME-1 cells into a nuclear and a cytoplasmic fraction.[23] Western analysis of the two fractions (Figure 1b) revealed that CBFβ–MYH11 and CBFβ are localized both in the cytoplasm as well as in the nucleus, whereas RUNX1 is primarily localized in the nucleus. These results suggest that CBFβ–MYH11 might indeed be involved in tethering some RUNX1 protein outside the nucleus, but that the vast majority of RUNX1 is still nuclear localized.

To identify CBFβ–MYH11-binding sites, we used two antibodies against CBFβ and two antibodies against MYH11 in ChIP-seq experiments (Figure 1c; Supplementary Figures S1A, B). The use of two antibodies for each of the fusion partners that each recognize a different epitope minimizes the risk of identifying nonspecific-binding sites that arise due to cross reactivity of the antibodies. Moreover, as wt MYH11 is not expressed in ME-1 cells,[24] the MYH11 antibodies allow specific identification of fusion protein binding. For all four tracks, we used model-based analysis of ChIP-Seq (MACS) with a *P*-value of 10^{-6} to identify signal enrichment. Overlapping the two antibodies for each of the fusion partners identified 11 517 CBFβ- and 2145 MYH11-binding sites (Figure 1d). Intersection of these two sets of binding regions allowed us to identify a set of 1874 regions (Supplementary Table S1) that are occupied with high confidence by the CBFβ–MYH11 oncofusion protein. A subset of these binding sites was validated through re-ChIP experiments on targeted loci, confirming that the two parts of the fusion protein occupy the same genomic region (Figure 1e). Moreover, ChIP-seq experiments using a specific antibody against RUNX1 revealed RUNX1 colocalization with CBFβ–MYH11 essentially at all high-confidence CBFβ–MYH11-binding regions (Figure 1c and Supplementary Figure S1C), reinforcing the suggestion that inv(16) leukemogenesis is RUNX1 dependent.

To validate the CBFβ–MYH11-binding regions, we used ChIP-seq to analyze the $CD34^+$ population of a newly diagnosed inv(16) patient. Because of the low amount of patient cells, we could only perform one ChIP-seq experiment with a CBFβ and one with a MYH11 antibody (Figure 1c; Supplementary Figure S1D). Nevertheless, this analysis showed increased tag density for both CBFβ as well as MYH11 at all of the high-confidence CBFβ–MYH11-binding sites (Figure 1f), thereby confirming the binding results obtained in the cell line. Comparing the genomic location of CBFβ–MYH11 with PML-RARα and AML1-ETO, two other AML-associated oncofusion proteins,[25,26] revealed a preferential localization of CBFβ–MYH11 to promoter regions as compared with AML1-ETO and PML-RARα, which both target mostly non-promoter regions (Figure 1g). To further evaluate this finding, we partitioned our newly discovered binding sites in three categories. One category containing the 1874 CBFβ–MYH11 (and RUNX1) binding regions, one containing all the CBFβ and RUNX1 occupied regions (CBFnoMYH) and one containing the RUNX1 only binding regions (RUNX1noCBF). Examining the genomic localization of these three categories revealed that ~75% of CBFβ–MYH11/RUNX1 and CBFβ/RUNX1 are enriched at transcription start sites, whereas 80% of RUNX1 only binding regions were non-promoter sites (Figure 1h), suggesting that CBFβ–MYH11 and CBFβ are mainly involved in regulating promoter activity, whereas RUNX1 can also regulate the activities of enhancer regions. Moreover, the results suggest that the interaction with RUNX1 alone cannot explain the localization of CBFβ and CBFβ–MYH11, as this would result in a different, more RUNX1-like genomic distribution. Hence additional factors are in place to guide CBFβ and CBFβ–MYH11 to promoter regions.

TAFs bind the CBFβ–MYH11/RUNX1 complex

Next we set out to assess which proteins act together with CBFβ–MYH11 in transcriptional regulation. As CBFβ–MYH11 *in vivo* is localized to RUNX1-binding sites, it allowed us to identify the CBFβ–MYH11 protein complex using DNA pull-down analysis followed by mass spectrometry. For this we performed DNA pull-down experiments using a specific nucleotide sequence bound by CBFβ–MYH11 in ME-1 cells (Supplementary Figure S2A) that contains the RUNX1 core consensus motif TGTGGT (RUNX1 oligo) and a control sequence with a scrambled RUNX1 motif (control oligo) (Figure 2a). We could show that the oligonucleotide with

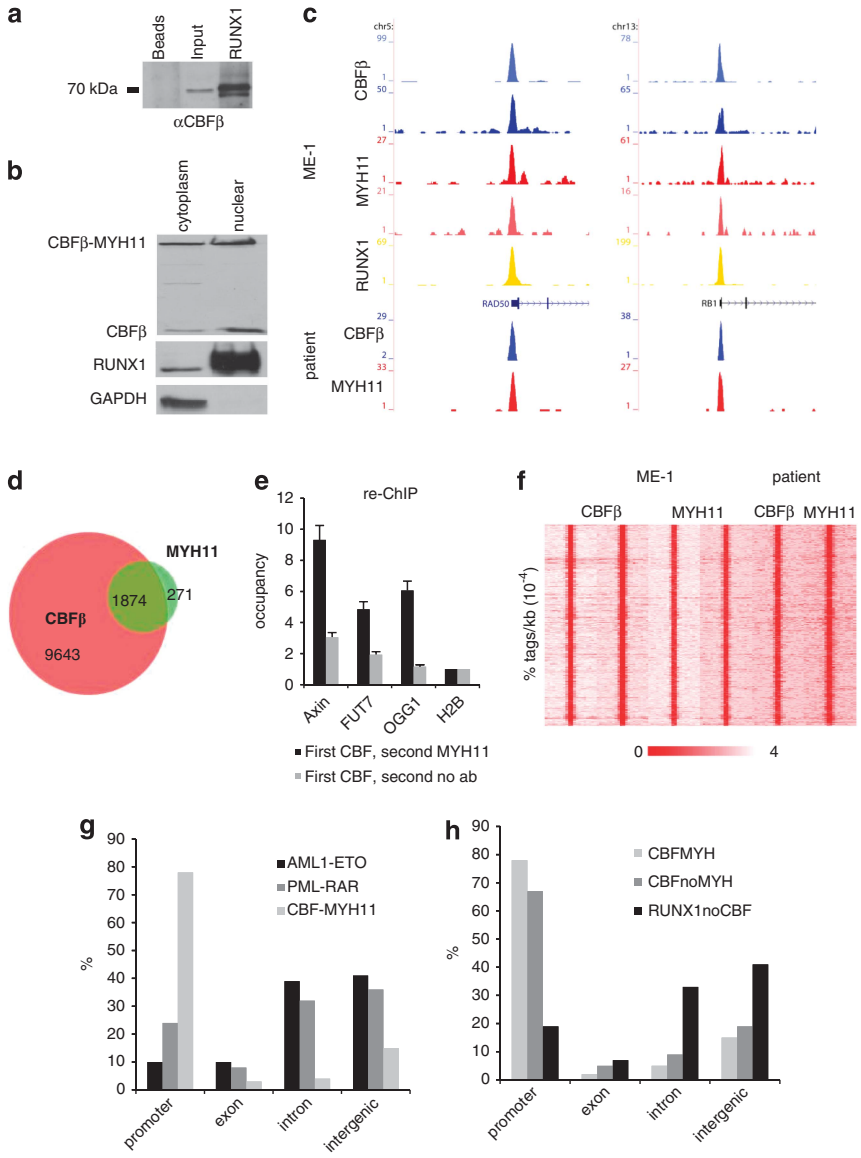

Figure 1. Genome-wide binding of CBFβ–MYH11. (**a**) Coimmunoprecipitation of CBFβ–MYH11 with RUNX1. Immunoprecipitations were performed in ME-1 cells using immunoglobulin G (beads) and RUNX1 antibodies and analyzed by western using CBFβ antibodies. (**b**) Western analysis of the cytoplasmic and nuclear fraction of ME-1 cells using antibodies recognizing CBFβ and RUNX1 and a control GAPDH antibody to validate the fractionation. (**c**) Overview of the *RAD50* and *RB1* CBFβ–MYH11-binding sites in ME-1 cells and a patient blast. In blue, the CBFβ ChIP-seq data are plotted, in red the MYH11 and in yellow the RUNX1 data. (**d**) Venn diagram representing the overlap of CBFβ and MYH111-binding sites in ME-1 cells. (**e**) Re-ChIP experiment validating CBFβ and MYH11 binding to the same locus. Three binding sites were selected and validated for CBFβ/MYH11 binding by re-chip using CBFβ antibodies in the first round of ChIP followed by a second round using MYH11 and no antibodies (**f**) Heat map displaying CBFβ and MYH11 tag densities in ME-1 an inv(16) patient cells at the high-confidence CBFβ–MYH11-binding sites identified in ME-1 cells. (**g**) Distribution of the CBFβ–MYH11, AML1-ETO and PML-RARα-binding site locations relative to RefSeq genes. Locations of binding sites are divided in promoter (− 500 bp to the transcription start site), exon, intron and intergenic (everything else). (**h**) Distribution of CBFβ–MYH11/RUNX1, CBFβ/RUNX1 and RUNX1-binding site locations relative to RefSeq genes. Location are as in (**g**).

the RUNX1 motif efficiently pulls down CBFβ–MYH11 as well as CBFβ from a ME-1 cell lysate, whereas the control sequence showed significantly reduced affinity for CBFβ–MYH11 (Figure 2b), confirming *in vitro* that CBFβ–MYH11 binding to DNA is largely RUNX1 dependent.

To characterize the interactome of the CBFβ–MYH11/RUNX1 complex, we used previously described SILAC-based technology,[21] using extracts derived from ME-1 cells grown in 'light' or 'heavy' medium, incubated with oligonucleotides containing the RUNX1 or a scrambled RUNX1 motif (see Materials and Methods). Of the >900 identified proteins, over 40 had highly significant ratios (>4) (Figure 2c; Supplementary Table S1) indicating specific binding to the CBFβ–MYH11/RUNX1 complex, whereas over 100 additional proteins, including previously identified RUNX1 interactors TAL1, FLI1 and BMI1,[27] had lower ratio's (>2) and might represent transient- or context-dependent interactions (Supplementary Table S1).

Interestingly, our pull-down analysis also suggested interaction of CBFβ–MYH11 with eight different TAFs (TBP-associated factors), TAF1, 3, 4, 5, 6, 7, 9 and 10 (Figure 2c; Supplementary Table S1). Subsequent coimmunoprecipitation experiments using ME-1 cells showed an interaction between CBFβ–MYH11 and TAF7

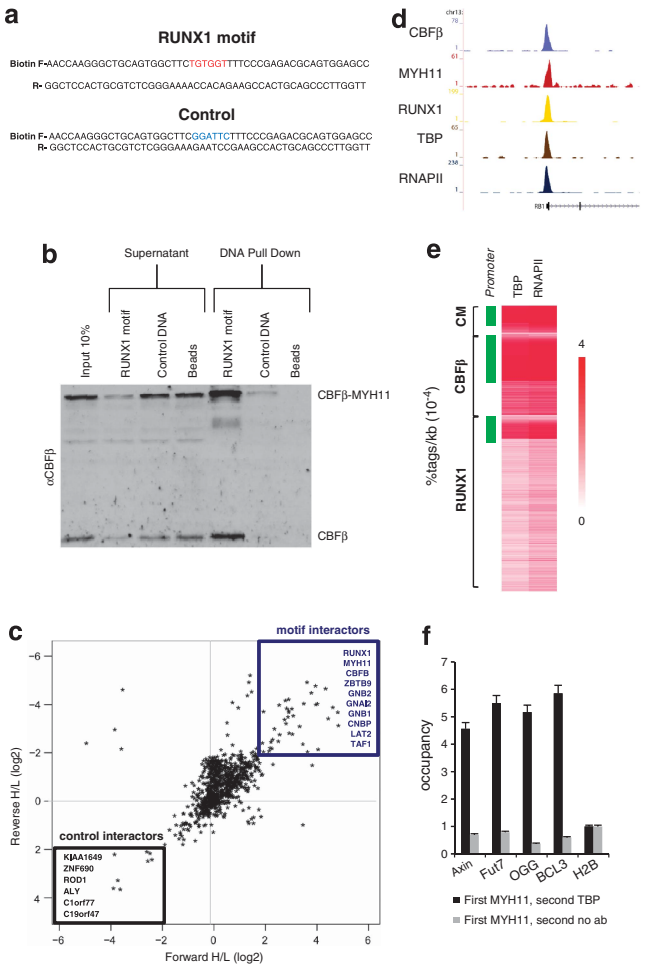

Figure 2. Identification of CBF complex components. (**a**) DNA sequence of the oligo's used in the pull-down analysis. (**b**) Western analysis of a DNA pulldown in ME-1 cells using a CBFβ antibody. CBFβ and CBFβ–MYH11 are enriched in the pulldown with the RUNX1 motif in comparison with the control. (**c**) Dotplot showing the result of the pull-down mass spectrometry experiment. Proteins are plotted by their SILAC-ratios in the forward (*x* axis) and reverse (*y* axis) SILAC experiment. Specific interactors of the RUNX1 pulldown lie in the upper right quadrant. (**d**) Overview of the *RB1* CBFβ–MYH11-binding site in ME-1 cells. (**e**) Heat map displaying TBP and RNAPII tag densities at high-confidence CBFβ–MYH11/RUNX1 (CM), CBFβ/RUNX1 (CBFβ) and RUNX1 only binding sites. Highest occupancy is observed at promoter regions bound by CBFβ–MYH11. (**f**) Re-ChIP experiment validating CBFβ–MYH11/TBP binding to the same locus. Three binding sites were selected and validated for CBFβ–MYH11/TBP binding by re-ChIP using MYH11 antibodies in the first round of ChIP followed by a second round using TBP and no antibodies.

(Supplementary Figure S2B), corroborating the pull-down results. Together these results suggest that interaction with TAFs might guide the localization of CBFβ or the fused CBFβ–MYH11 to promoter sites.

As TAFs form a stable complex with TBP and RNAPII to form a preinitiation complex, we wondered whether *in vivo* these two factors would bind similar genomic regions as the CBFβ–MYH11 complex. Indeed, genome-wide analysis revealed the occupancy of CBFβ–MYH11/RUNX1, TBP and RNAPII at similar genomic regions (Figure 2d). Moreover, further analysis of TBP and RNAPII occupancy at CBFβ–MYH11 (CM) regions as compared with RUNX1/CBFβ (CBFβ) and RUNX1 only regions revealed highest levels of TBP and RNAPII at CBFβ–MYH11 sites located in promoter regions (Figure 2e).

To further validate that they bind the same genomic regions, we performed re-ChIP experiments. This confirmed TBP and CBFβ–MYH11 binding to the same genomic loci (Figure 2f). Together these results suggest that the CBFβ–MYH11/RUNX1 complex interacts with basal transcriptional factors and occupies similar genomic regions.

CBFβ–MYH11/RUNX1 bound regions are occupied by ETS factors, TAL1, GATA2 and HEB

To examine whether CBFβ–MYH11-binding sites harbor specific DNA elements, we investigated the presence of consensus binding motifs for various hematopoietic regulators such as E-box proteins, GATA and ETS factors, TAL1 and RUNX. This analysis revealed that most binding sites harbor DNA motifs for RUNX1, ETS and E-box factors (Figure 3a), while also TAL1, GATA and NFκB consensus binding sequences can be found in a high number of sites. These results suggest that CBFβ–MYH11 might function in the context of other hematopoietic regulators.

The pull-down analysis suggested interaction of the CBF complex with TAL1 and the ETS factor FLI1, in line with the presence of the RUNX1, ETS and TAL1 motif at CBFβ–MYH11-binding sites. Our motif analysis further revealed the presence of the E-box and GATA motif at CBFβ–MYH11-binding sites. To investigate whether TAL1, E-box and GATA factors are present at CBFβ–MYH11 bound regions, we extended our ChIP-seq analysis and included specific antibodies to TAL1, GATA2, the GATA factor highest expressed in ME-1 cells, HEB, a protein previously implicated in CBF leukemogenesis,[26,28,29] and also included several ETS factors, such as ELF1, FLI1, ERG and PU.1/SPI1 in our analysis. This revealed the increased occupancy of all factors at the CBFβ–MYH11/RUNX1 occupied promoters of the *C8ORF55* and *SOCS1* genes (Figure 3b) whereas, in contrast, not all factors were enriched at the CBFβ/RUNX1 occupied *TAL1* or RUNX1 occupied *PSMC3* gene. For all transcription factors, we identified the genome-wide binding regions using model-based analysis of ChIP-Seq (MACS), and the resulting peak files were, together with the different sets of CBF-binding sites (CBFβ–MYH11/RUNX1, CBFβ/RUNX1 and RUNX1 only), used as input for unsupervised segmentation analysis using ChromHMM.[30] ChromHMM is based on a multivariate hidden Markov model that allows modeling of the presence or absence of a transcription factor by integrating multiple data sets to discover *de novo* the major re-occurring combinatorial and spatial patterns of transcription factors. Here, it allowed the identification of 23 distinct transcription factor co-occupancy patterns within the inv(16) cells (Figure 3c). In line with our observations at the *TAL1* and *PSMC3* genes, various transcription factor patterns could be detected at CBFβ/RUNX1 or at RUNX1 only occupied regions (Figure 3c). In contrast, at the CBFβ–MYH11/RUNX1 occupied regions (state 9), enrichment for all transcription factors was found (Figure 3c and Supplementary Figure S3), suggesting that CBFβ–MYH11 functions in the context of many other hematopoietic transcription factors.

To further validate that CBFβ–MYH11 binds the same genomic regions as other hematopoietic regulators, we performed re-ChIP experiments. This confirmed that ELF1, FLI1, PU.1, ERG and CBFβ–MYH11 bind the same genomic locus (Figure 3d).

HATs and HDACs regulate CBFβ–MYH11 occupied regions

CBFβ–MYH11 has been reported to recruit HDACs to its target sites,[31] similar as for other oncofusion proteins such as AML1-ETO and PML-RARα. To assess whether CBFβ–MYH11 binding correlates with histone (de)acetylation, we performed ChIP-seq analysis using an antibody that recognizes H3 acetylation. Examining the average profile of this histone mark at our previously defined binding sites revealed highest H3 acetylation

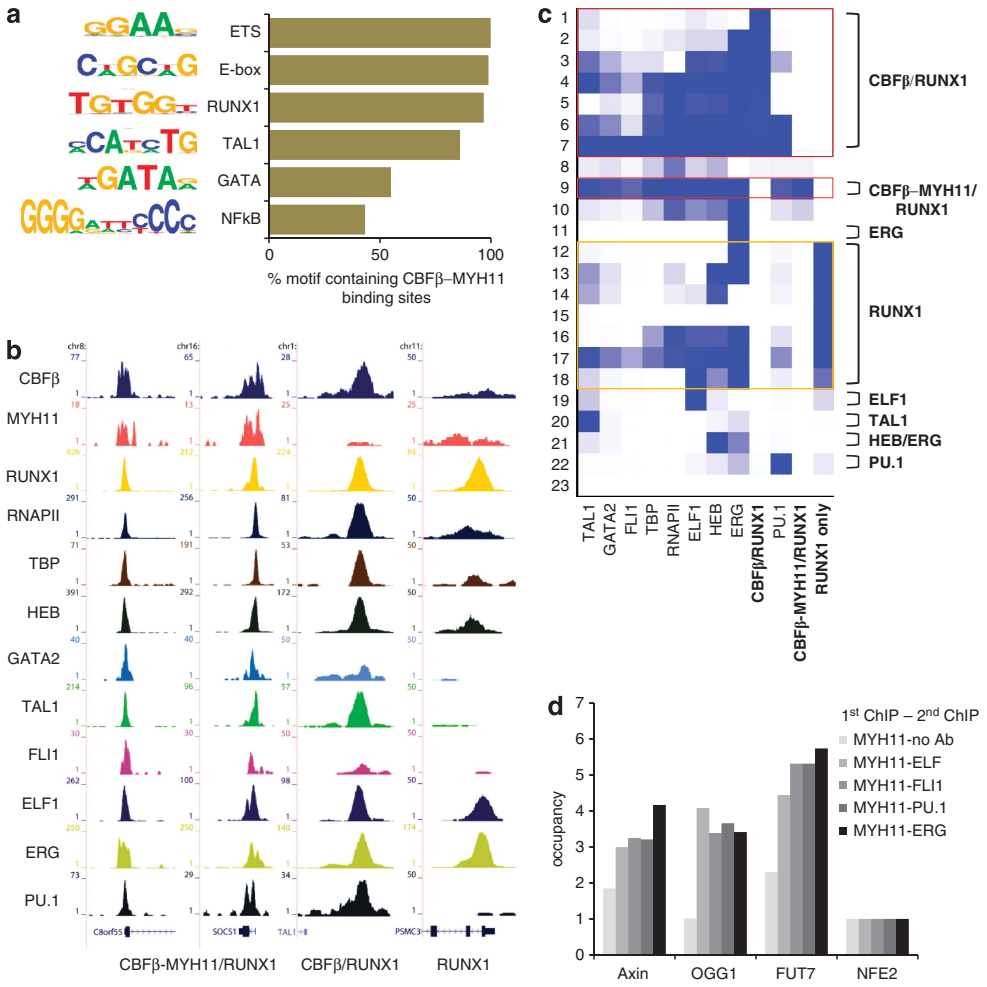

Figure 3. Transcription factor occupancy at CBFβ–MYH11-binding sites. (**a**) Diagram depicting the percentage of CBFβ–MYH11-binding sites harboring a hematopoietic regulator consensus binding sequences. (**b**) Overview of the *C8ORF55* and *SOCS1* CBFβ–MYH11/RUNX1, the *TAL1* CBFβ/RUNX1 and the *PSMC3* RUNX1-binding site in ME-1 cells. ChIP-seq data are plotted for CBFβ, MYH11, RUNX1, RNAPII, TBP, HEB, GATA2, TAL1, FLI1, ELF1, ERG and PU.1. (**c**) ChromHMM segmentation analysis of the transcription factor binding sites in ME-1 cells. (**d**) Re-ChIP experiment validating CBFβ–MYH11/TF binding to the same locus. Three binding sites were selected and validated for CBFβ–MYH11/TF binding by re-chip using MYH11 antibodies in the first round of ChIP followed by a second round using ELF, FLI1, PU.1, ERG and no antibodies.

at the 1874 CBFβ–MYH11/RUNX1-binding sites (CBFMYH11), whereas the sets of unique CBFβ/RUNX1 (CBF) and RUNX1 only sites harbor lower levels of H3 acetylation (Figure 4a).

Histone acetylation levels have been suggested to be the result of the dynamic interplay of histone acetyl tranferases (HATs) and histone deacetylases (HDACs).[32–35] To examine whether both enzymatic activities are recruited to CBFβ–MYH11 sites, we performed ChIP-seq using specific antibodies against HDAC1 and the HAT EP300. This analysis revealed the presence of both EP300 and HDAC1 at the CBFβ–MYH11 sites at the HDAC1 and HM13 genes (Figure 4b). Intersection of the EP300 and HDAC1 sites confirmed that on a genome-wide scale both HAT and HDAC activities are recruited together at many sites (Figure 4c). Examining the occupancy of EP300 and HDAC1 as well as H3 acetylation specifically at all CBFβ–MYH11-binding sites revealed increased levels at all high-confidence sites (Figure 4d). Together these results suggest that H3 acetylation levels at CBFβ–MYH11 are the result of the activities of counteracting HAT and HDAC proteins.

CBFβ–MYH11 binds at the promoters of active genes

As our results reveal that CBFβ–MYH11 (and CBFβ) targets promoter regions that harbor increased H3 acetylation, we wondered whether CBFβ–MYH11 target genes are expressed. For this we assigned genes to each binding site and analyzed the expression of these target genes through RNA-seq. RPKM (reads per kilobase exon per million tags sequenced) analysis revealed that although the expression of genes associated with CBFβ–MYH11/RUNX1 occupied promoters can vary extensively (Figure 5a, outer whiskers in boxplot), RPKM values are generally higher in this context than for genes that bind only CBFβ/RUNX1 (CBFβ) or RUNX1. As RPKM measurements are derived from RNA, which could have been alternatively regulated through post transcriptional processes, we decided to also examine RNAPII occupancy as a measurement for ongoing transcription.[36] Analysis of the same gene sets revealed highest RNAPII occupancy at genes targeted by CBFβ–MYH11 (Figure 5b), whereas CBFβ/RUNX1 and RUNX1 only target genes have reduced RNAPII occupancy.

Finally, we analyzed the expression status using available microarray expression data[37] of the target genes in patients ($n = 33$) harboring an inv(16) translocation. This analysis confirmed that CBFβ–MYH11 target genes are higher expressed than CBFβ/RUNX1 or RUNX1 only target genes (Figure 5c). Together, these results suggest that although CBFβ–MYH11 has been suggested to repress transcriptional activity, CBFβ–MYH11 binding can also be associated with gene activity.

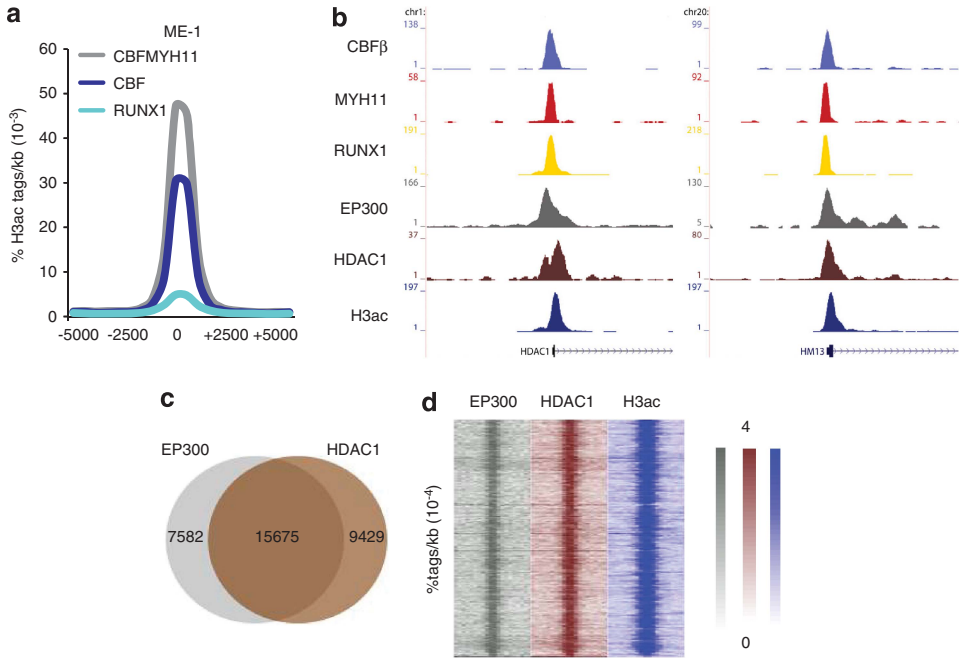

Figure 4. CBFβ–MYH11 occupied regions are hyperacetylated. (**a**) Median H3 acetylation profile over CBFβ–MYH11/RUNX1, CBFβ/RUNX1 (CBF) and RUNX1-binding sites. (**b**) Overview of the *HDAC1* and *HM13* CBFβ–MYH11-binding sites in ME-1 cells, showing the binding of both EP300 and HDAC1 as well as increased levels of H3 acetylation. (**c**) Venn diagram representing the overlap of EP300- and HDAC1-binding sites in ME-1 cells. (**d**) Heat map displaying EP300, HDAC1 and H3ac tag densities at high-confidence CBFβ–MYH11-binding sites.

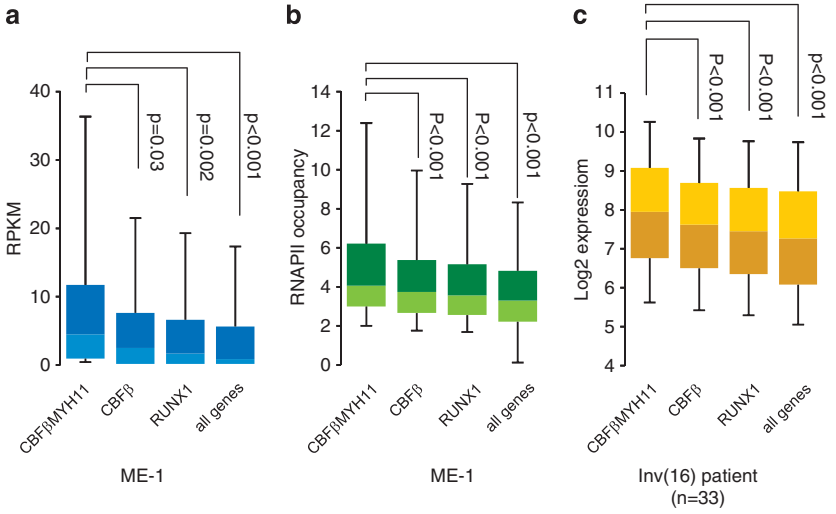

Figure 5. CBFβ–MYH11 occupied regions correlate with increased gene activity. (**a**) Boxplot showing RPKM values of CBFβ–MYH11/RUNX1, CBFβ/RUNX1 (CBFβ) and RUNX1 target genes in ME-1 cells. (**b**) Boxplot showing RNAPII tag density at CBFβ–MYH11/RUNX1, CBFβ/RUNX1 and RUNX1 target genes in ME-1 cells. (**c**) Boxplot showing log2 expression values of CBFβ–MYH11/RUNX1, CBFβ/RUNX1 and RUNX1 target genes in inv(16) patient blasts ($n = 33$).

CBFβ–MYH11 is involved in gene activation and repression

To further examine the effects of CBFβ–MYH11 binding on gene expression, we made use of an inducible U937 cell line that upon tetracycline (Tet) depletion expressed CBFβ–MYH11 (Tet-off).[38] Indeed, 72 h after Tet was removed the expression of CBFβ–MYH11 was detected both at the level of RNA (Figure 6a) and protein (Figure 6b), although lower as observed in the ME-1 cell line. ChIP-seq using antibodies against CBFβ and MYH11 after CBFβ–MYH11 expression allowed the identification of 2312 novel binding sites occupied by both CBFβ and MYH11 (Figure 6c). Assigning these binding sites to genes and subsequent RNA-seq analysis revealed that, of the 263 genes twofold or more upregulated or downregulated, 67% are twofold or more upregulated (Figure 6d), whereas 33% are lowly expressed, suggesting that CBFβ–MYH11 is involved both in transcriptional activation and repression.

To examine the effect of CBFβ–MYH11 knockdown on inv(16) cells, we constructed a CBFβ–MYH11 inducible knockdown system using ME-1 cells. Reverse transcription-quantitative PCR and western analysis of ME-1 cells carrying an inducible CBFβ–MYH11 knockdown construct revealed, after induction, decreased RNA and protein levels of CBFβ–MYH11 in the ME-1 cells carrying

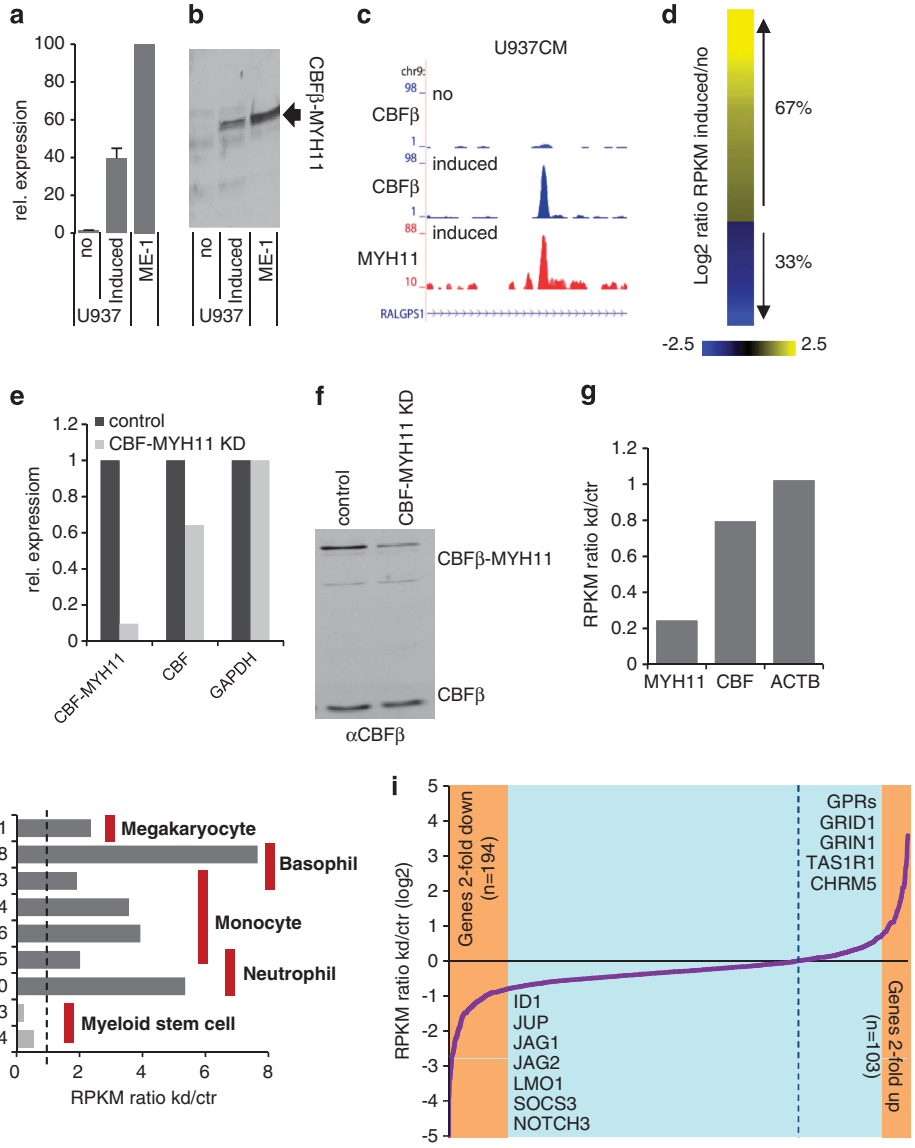

Figure 6. CBFβ–MYH11 is involved in gene activation and repression. (**a**) Reverse transcription-quantitative PCR (RT-qPCR) analysis of CBFβ–MYH11 expression in U937 TET inducible CBFβ–MYH11 cells (U937CM) and ME-1 cells. (**b**) Western blot analysis of CBFβ–MYH11 expression in U937 TET inducible CBFβ–MYH11 (U937CM) and ME-1 cells. (**c**) Overview of the *RALGPS1* CBFβ–MYH11-binding site in U937CM cells. In blue the CBFβ ChIP-seq data are plotted in induced and uninduced U937CM cells and in red the MYH11 ChIP-seq data in induced U937CM cells. (**d**) Heatmap display of the log2 ratio of CBFβ–MYH11 target genes after and before the induction of oncofusion protein expression. Only results for the 263 genes twofold or more up- or downregulated are shown. (**e**) RT-qPCR analysis of CBFβ–MYH11 and CBFβ expression in ME-1 cells expressing a CBFβ–MYH11 knockdown hairpin without (control) or after induction. (**f**) Western analysis of CBFβ–MYH11 and CBFβ expression in ME-1 cells expressing a CBFβ–MYH11 knockdown hairpin without and after induction. (**g**) RNA-seq-based RPKM ratio of CBFβ–MYH11 (MYH11), CBFβ (CBF) and β-actin (ACTB) of CBFβ–MYH11 knockdown ME-1 cells versus an uninduced control. (**h**) RPKM ratio of various CD markers of CBFβ–MYH11 knockdown ME-1 cells versus an uninduced control. The cell type for which the CD markers are indicative are mentioned on the right. (**i**) RPKM ratio of CBFβ–MYH11 knockdown ME-1 cells versus an uninduced control of all CBFβ–MYH11 target genes. A total of 194 target genes are twofold or more downregulated and 103 target genes are more then twofold upregulated after CBFβ–MYH11 knockdown.

the knockdown hairpin (Figures 6e and f). Subsequent genome-wide transcriptome analysis using RNA-seq confirmed lower *CBFβ–MYH11* RPKM levels after knockdown (Figure 6g).

Upon CBFβ–MYH11 knockdown, we observed increased attachment of cells to the culture dish suggesting the initiation of a differentiation/cell adherens program (Supplementary Figure S4A). To further assess this knockdown phenotype, we examined the expression of CD markers. This revealed that ME-1 cells with lowered CBFβ–MYH11 have decreased levels of myeloid stem cell marker genes such as *CD34* and *CD133* (Figure 6h), whereas various markers for differentiated myeloid cell types are increased (Figure 6h; Supplementary Table S1), suggesting that CBFβ–MYH11 knockdown results in a more differentiated myeloid phenotype. In addition, we examined which CBFβ–MYH11 target genes are differential expressed upon CBFβ–MYH11 knockdown. Using a twofold change cutoff, 194 genes were identified for which the expression is lower upon knockdown, whereas 103 CBFβ–MYH11 target genes are higher expressed (Figure 6i; Supplementary Table S1), suggesting that the oncofusion protein is involved both in gene expression and repression. Apart from

CBFβ–MYH11 target genes also many CBFβ/RUNX1 and RUNX1 only target genes were differentially expressed (Supplementary Figure S4B; Supplementary Table S1), suggesting that the effects of CBFβ–MYH11 extend to the complete CBF gene network.

Although for the CBFβ–MYH11 target genes that were highly expressed, many receptors, such as *GPRs, CHRM5, GRIN1* and *GRID1*, were detected (Figure 6i), genes that were lower expressed include suppressors of cytokine signaling (*SOCS3*) and members of the WNT (*JUP*) and NOTCH (*JAG1, JAG2* and *NOTCH3*) pathways (Supplementary Figure S4C). Interestingly, *JAG1*, but also *LMO1* and *ID1,* have been implicated in hematopoietic stem cell expansion,[39–42] suggesting that reduced expression of these genes in CBFβ–MYH11 knockdown cells affects its self-renewal capacity. Indeed, hypergeometric testing of a combined set of self-renewal pathways involved in myeloid malignancies[43] revealed significant enrichment (*P*-value $1.59e^{-4}$) (Supplementary Figure S4C) for genes downregulated upon CBFβ–MYH11 knockdown.

DISCUSSION

Many breakpoints involved in specific chromosomal translocations have been cloned over the years. In most cases, however, the role of the chimeric oncofusion proteins in tumorigenesis has not been elucidated. In the case of AML, our analysis of PML-RARα and AML1-ETO were among the first to report on the genome-wide actions of oncofusion proteins.[25,26,44] Here, we analyzed the genome-wide-binding pattern of CBFβ–MYH11 and its interplay with other regulators of hematopoiesis in cell lines and patient primary blasts.

As CBFβ–MYH11 has been suggested to localize primarily in the cytoplasm[45,46] thereby tethering RUNX1 outside the nucleus, we first examined the cellular localization of both proteins through fractionation experiments. This revealed CBFβ–MYH11 presence both in the cytoplasm as well as in the nucleus, whereas RUNX1 was predominantly localized in the nucleus, suggesting that CBFβ–MYH11 could tether some RUNX1 outside the nucleus, but that it also has a role within the nucleus.

To identify CBFβ–MYH11 binding, we used two antibodies specifically recognizing the CBFβ part as well as two antibodies recognizing the MYH11 part of the CBFβ–MYH11 protein in ChIP-seq and identified 1874 high confidence, mostly promoter binding sites in ME-1 cells. In addition, we analyzed genome-wide CBFβ-MYH11 binding in a patient blast and could validate enrichments of both CBFβ and MYH11 at all high-confidence binding sites. Moreover, we could detect RUNX1 at all CBFβ–MYH11-binding sites in line with previous reports suggesting that the presence of RUNX1 is required for CBFβ–MYH11 binding.

We used a SILAC-based mass spectrometry approach to identify components of the CBFβ–MYH11 complex and confirmed previous observations on the presence of TAL1 and FLI1 in the CBF RUNX1/CBFβ complex. In addition, the interaction study revealed the presence of eight TAFs. As CBFβ–MYH11 localizes primarily to promoter regions, these results suggest that the preferential localization of CBFβ–MYH11 to promoters may be a result of the interaction with TAFs.

The presence of binding motifs for all major hematopoietic regulators in CBFβ–MYH11-binding regions prompted further investigation on the presence of hematopoietic regulators. This investigation, which included the analysis using specific HEB, GATA2, ERG, PU.1 and ELF1 antibodies in ChIP-seq, revealed the presence of all these important regulators at CBFβ–MYH11 occupied regions. Although it was previously suggested that CBFβ–MYH11 interferes with the RUNX1 transcription program through steric hindrance of transcription factor complex assembly[4,5] the MYH11 moiety of CBFβ–MYH11 apparently does not preclude the interaction and co-occupancy of the transcription factors examined in this study.

In addition, our analysis revealed that at the epigenetic level CBFβ–MYH11 occupied regions are enriched for H3 acetylation and most likely regulated by the balanced interplay of the antagonistic activities of histone-modifying enzymes such as HATs and HDACs (but most likely also methyltransferases and demethylases).[32–35] Together these results suggest that genes important for maintaining leukemogenic potential (as evident from the targeting of CBFβ–MYH11 to these regions) are regulated by many different transcription factors and coregulators and that most likely their interplay determines the transcriptional output.

Previously, CBFβ–MYH11 has been proposed to act as a transcriptional repressor of its target genes. To assess this, we examined the expression of CBFβ–MYH11 target genes in the ME-1 inv(16) cell line, in a U937 cell line harboring an inducible CBFβ–MYH11 construct and in patient cells. Comparing all genes targeted by CBFs (CBFβ–MYH11/RUNX1, CBFβ/RUNX1 and RUNX1 only), we found those that have CBFβ–MYH11 binding to be on average the highest expressed, whereas those genes bound by CBFβ/RUNX1 or RUNX1 alone were lowly expressed, suggesting a role for CBFβ–MYH11 in transcriptional activation. CBFβ–MYH11 overexpression as well as knockdown confirmed that subsets of target genes are repressed by the oncofusion protein, but that for a large set CBFβ–MYH11 is involved in maintaining increased transcriptional activity. What causes this difference is currently unclear, but it might be dependent on the presence of not yet identified proteins, interactions with enhancer elements, signaling cascades and/or spatial localization. Among the genes that are actively transcribed in inv(16) cells and repressed after CBFβ–MYH11 knockdown are *JAG1*, *LMO1* and *ID1*. Interestingly, enforced expression of *LMO1* induces leukemia's,[39] and *LMO1* null mutations in mice can lead to severe reduction of steady-state hematopoietic stem cell numbers,[41] a phenotype also observed in ID1-deficient hematopoietic stem cells.[42] Finally, inducing JAG1 expression results in the expansion of hematopoietic precursor cell populations,[39] suggesting that reduced expression of these genes in CBFβ–MYH11 knockdown cells affects their self-renewal capacity.

CONFLICT OF INTEREST

The authors declare no conflict of interest.

ACKNOWLEDGEMENTS

We thank E Megens, K Berentsen and M Bergsma for assistance, C Logie for discussion and H Kerstens, S van Heeringen, A Brinkman and K Francoijs for bioinformatic support. U937-CBFβ–MYH11 cells were a kind gift of T Pabst. This work was supported by the EU (ATLAS-221952; BLUEPRINT-282510), the Dutch Cancer Foundation (KWF KUN 2009-4527 and KUN 2011-4937) and the Netherlands Organization for Scientific Research (NWO-VIDI to JM).

AUTHOR CONTRIBUTIONS

The work presented here was carried out in collaboration between all authors. JHAM, AM, AS, PJ, AW, HR, FG, KP, SS, EV, MV and HGS designed methods and performed the experiments. JHAM, AM, AS, MV and HGS interpreted the results and wrote the manuscript and all authors contributed to the manuscript preparation. All authors have contributed to, seen, and approved the manuscript.

DATABASE ACCESSION

All ChIP-seq and RNA-seq data can be downloaded from the NCBI Gene Expression Omnibus (GEO) (http://www.ncbi.nlm.nih.gov/geo/) under accession number GSE46044.

REFERENCES

1 Appleford PJ, Woollard A. RUNX genes find a niche in stem cell biology. *J Cell Biochem* 2009; **108**: 14–21.
2 Zeisig BB, Kulasekararaj AG, Mufti GJ, So CW. SnapShot: acute myeloid leukemia. *Cancer Cell* 2012; **22**: 698–698, e691.

3 Nimer SD, Moore MA. Effects of the leukemia-associated AML1-ETO protein on hematopoietic stem and progenitor cells. *Oncogene* 2004; **23**: 4249–4254.
4 Shigesada K, van de Sluis B, Liu PP. Mechanism of leukemogenesis by the inv(16) chimeric gene CBFB/PEBP2B-MHY11. *Oncogene* 2004; **23**: 4297–4307.
5 Liu P, Tarle SA, Hajra A, Claxton DF, Marlton P, Freedman M *et al.* Fusion between transcription factor CBF beta/PEBP2 beta and a myosin heavy chain in acute myeloid leukemia. *Science* 1993; **261**: 1041–1044.
6 Springall FH, Lukeis RL, Tyrrell V, Joshua DE, Iland HJ. Identification of a novel CBFB-MYH11 fusion transcript in a patient with AML and inversion of chromosome 16. *Leukemia* 1998; **12**: 2034–2035.
7 Schnittger S, Bacher U, Haferlach C, Kern W, Haferlach T. Rare CBFB-MYH11 fusion transcripts in AML with inv(16)/t(16;16) are associated with therapy-related AML M4eo, atypical cytomorphology, atypical immunophenotype, atypical additional chromosomal rearrangements and low white blood cell count: a study on 162 patients. *Leukemia* 2007; **21**: 725–731.
8 Boeckx N, De Roover J, van der Velden VH, Maertens J, Uyttebroeck A, Vandenberghe P *et al.* Quantification of CBFB-MYH11 fusion gene levels in paired peripheral blood and bone marrow samples by real-time PCR. *Leukemia* 2005; **19**: 1988–1990.
9 Castilla LH, Wijmenga C, Wang Q, Stacy T, Speck NA, Eckhaus M *et al.* Failure of embryonic hematopoiesis and lethal hemorrhages in mouse embryos heterozygous for a knocked-in leukemia gene CBFB-MYH11. *Cell* 1996; **87**: 687–696.
10 Okuda T, van Deursen J, Hiebert SW, Grosveld G, Downing JR. AML1, the target of multiple chromosomal translocations in human leukemia, is essential for normal fetal liver hematopoiesis. *Cell* 1996; **84**: 321–330.
11 Wang Q, Stacy T, Miller JD, Lewis AF, Gu TL, Huang X *et al.* The CBFbeta subunit is essential for CBFalpha2 (AML1) function *in vivo*. *Cell* 1996; **87**: 697–708.
12 Castilla LH, Garrett L, Adya N, Orlic D, Dutra A, Anderson S *et al.* The fusion gene Cbfb-MYH11 blocks myeloid differentiation and predisposes mice to acute myelomonocytic leukaemia. *Nat Genet* 1999; **23**: 144–146.
13 Castilla LH, Perrat P, Martinez NJ, Landrette SF, Keys R, Oikemus S *et al.* Identification of genes that synergize with Cbfb-MYH11 in the pathogenesis of acute myeloid leukemia. *Proc Natl Acad Sci USA* 2004; **101**: 4924–4929.
14 Speck NA, Gilliland DG. Core-binding factors in haematopoiesis and leukaemia. *Nat Rev Cancer* 2002; **2**: 502–513.
15 Van der Reijden BA, Massop M, Simons A, de Witte T, Breuning M, Jansen JH. The NDE1 gene is disrupted by the inv(16) in 90% of cases with CBFB-MYH11-positive acute myeloid leukemia. *Leukemia* 2010; **24**: 857–859.
16 Haferlach C, Dicker F, Kohlmann A, Schindela S, Weiss T, Kern W *et al.* AML with CBFB-MYH11 rearrangement demonstrate RAS pathway alterations in 92% of all cases including a high frequency of NF1 deletions. *Leukemia* 2010; **24**: 1065–1069.
17 Zhao L, Melenhorst JJ, Alemu L, Kirby M, Anderson S, Kench M *et al.* KIT with D816 mutations cooperates with CBFB-MYH11 for leukemogenesis in mice. *Blood* 2011; **119**: 1511–1521.
18 Liu PP, Hajra A, Wijmenga C, Collins FS. Molecular pathogenesis of the chromosome 16 inversion in the M4Eo subtype of acute myeloid leukemia. *Blood* 1995; **85**: 2289–2302.
19 Lutterbach B, Hou Y, Durst KL, Hiebert SW. The inv(16) encodes an acute myeloid leukemia 1 transcriptional corepressor. *Proc Natl Acad Sci USA* 1999; **96**: 12822–12827.
20 Wee HJ, Voon DC, Bae SC, Ito Y. PEBP2-beta/CBF-beta-dependent phosphorylation of RUNX1 and p300 by HIPK2: implications for leukemogenesis. *Blood* 2008; **112**: 3777–3787.
21 Spruijt CG, Gnerlich F, Smits AH, Pfaffeneder T, Jansen PW, Bauer C *et al.* Dynamic readers for 5-(hydroxy)methylcytosine and its oxidized derivatives. *Cell* 2013; **152**: 1146–1159.
22 Yanagisawa K, Horiuchi T, Fujita S. Establishment and characterization of a new human leukemia cell line derived from M4E0. *Blood* 1991; **78**: 451–457.
23 Andrews NC, Faller DV. A rapid micropreparation technique for extraction of DNA-binding proteins from limiting numbers of mammalian cells. *Nucleic Acids Res* 1991; **19**: 2499.
24 van der Reijden BA, Massop M, Tonnissen E, van de Locht L, Muus P, de Witte T *et al.* Rapid identification of CBFB-MYH11-positive acute myeloid leukemia (AML) cases by one single MYH11 real-time RT-PCR. *Blood* 2003; **101**: 5085–5086.
25 Martens JH, Brinkman AB, Simmer F, Francoijs KJ, Nebbioso A, Ferrara F *et al.* PML-RARalpha/RXR alters the epigenetic landscape in acute promyelocytic leukemia. *Cancer Cell* 2010; **17**: 173–185.
26 Martens JH, Mandoli A, Simmer F, Wierenga BJ, Saeed S, Singh AA *et al.* ERG and FLI1 binding sites demarcate targets for aberrant epigenetic regulation by AML1-ETO in acute myeloid leukemia. *Blood* 2012; **120**: 4038–4048.
27 Yu M, Mazor T, Huang H, Huang HT, Kathrein KL, Woo AJ *et al.* Direct recruitment of polycomb repressive complex 1 to chromatin by core binding transcription factors. *Mol Cell* 2012; **45**: 330–343.
28 Gardini A, Cesaroni M, Luzi L, Okumura AJ, Biggs JR, Minardi SP *et al.* AML1/ETO oncoprotein is directed to AML1 binding regions and co-localizes with AML1 and HEB on its targets. *PLoS Genet* 2008; **4**: e1000275.
29 Zhang J, Kalkum M, Yamamura S, Chait BT, Roeder RG. E protein silencing by the leukemogenic AML1-ETO fusion protein. *Science* 2004; **305**: 1286–1289.
30 Ernst J, Kellis M. ChromHMM: automating chromatin-state discovery and characterization. *Nat Methods* 2012; **9**: 215–216.
31 Durst KL, Lutterbach B, Kummalue T, Friedman AD, Hiebert SW. The inv(16) fusion protein associates with corepressors via a smooth muscle myosin heavy-chain domain. *Mol Cell Biol* 2003; **23**: 607–619.
32 Saeed S, Logie C, Francoijs KJ, Frige G, Romanenghi M, Nielsen FG *et al.* Chromatin accessibility, p300, and histone acetylation define PML-RARalpha and AML1-ETO binding sites in acute myeloid leukemia. *Blood* 2012; **120**: 3058–3068.
33 Agrawal-Singh S, Isken F, Agelopoulos K, Klein HU, Thoennissen NH, Koehler G *et al.* Genome-wide analysis of histone H3 acetylation patterns in AML identifies PRDX2 as an epigenetically silenced tumor suppressor gene. *Blood* 2012; **119**: 2346–2357.
34 Whyte WA, Bilodeau S, Orlando DA, Hoke HA, Frampton GM, Foster CT *et al.* Enhancer decommissioning by LSD1 during embryonic stem cell differentiation. *Nature* 2012; **482**: 221–225.
35 Wang Z, Zang C, Cui K, Schones DE, Barski A, Peng W *et al.* Genome-wide mapping of HATs and HDACs reveals distinct functions in active and inactive genes. *Cell* 2009; **138**: 1019–1031.
36 Welboren WJ, van Driel MA, Janssen-Megens EM, van Heeringen SJ, Sweep FC, Span PN *et al.* ChIP-Seq of ERalpha and RNA polymerase II defines genes differentially responding to ligands. *EMBO J* 2009; **28**: 1418–1428.
37 Verhaak RG, Wouters BJ, Erpelinck CA, Abbas S, Beverloo HB, Lugthart S *et al.* Prediction of molecular subtypes in acute myeloid leukemia based on gene expression profiling. *Haematologica* 2009; **94**: 131–134.
38 Helbling D, Mueller BU, Timchenko NA, Schardt J, Eyer M, Betts DR *et al.* CBFB-SMMHC is correlated with increased calreticulin expression and suppresses the granulocytic differentiation factor CEBPA in AML with inv(16). *Blood* 2005; **106**: 1369–1375.
39 Chervinsky DS, Zhao XF, Lam DH, Ellsworth M, Gross KW, Aplan PD. Disordered T-cell development and T-cell malignancies in SCL LMO1 double-transgenic mice: parallels with E2 A-deficient mice. *Mol Cell Biol* 1999; **19**: 5025–5035.
40 Varnum-Finney B, Purton LE, Yu M, Brashem-Stein C, Flowers D, Staats S *et al.* The Notch ligand, Jagged-1, influences the development of primitive hematopoietic precursor cells. *Blood* 1998; **91**: 4084–4091.
41 Zhu J, Emerson SG. Hematopoietic cytokines, transcription factors and lineage commitment. *Oncogene* 2002; **21**: 3295–3313.
42 Jankovic V, Ciarrocchi A, Boccuni P, DeBlasio T, Benezra R, Nimer SD. Id1 restrains myeloid commitment, maintaining the self-renewal capacity of hematopoietic stem cells. *Proc Natl Acad Sci USA* 2007; **104**: 1260–1265.
43 Sands WA, Copland M, Wheadon H. Targeting self-renewal pathways in myeloid malignancies. *Cell Commun Signal* 2013; **11**: 33.
44 Ptasinska A, Assi SA, Mannari D, James SR, Williamson D, Dunne J *et al.* Depletion of RUNX1/ETO in t(8;21) AML cells leads to genome-wide changes in chromatin structure and transcription factor binding. *Leukemia* 2012; **26**: 1829–1841.
45 Adya N, Stacy T, Speck NA, Liu PP. The leukemic protein core binding factor beta (CBFbeta)-smooth-muscle myosin heavy chain sequesters CBFalpha2 into cytoskeletal filaments and aggregates. *Mol Cell Biol* 1998; **18**: 7432–7443.
46 Kanno Y, Kanno T, Sakakura C, Bae SC, Ito Y. Cytoplasmic sequestration of the polyomavirus enhancer binding protein 2 (PEBP2)/core binding factor alpha (CBFalpha) subunit by the leukemia-related PEBP2/CBFbeta-SMMHC fusion protein inhibits PEBP2/CBF-mediated transactivation. *Mol Cell Biol* 1998; **18**: 4252–4261.

Supplementary Information accompanies this paper on the Leukemia website (http://www.nature.com/leu)